# Drying of a colloidal suspension deposited on a substrate: experimental and numerical studies

Nathalie Olivi-Tran, Laurent Bonnet, Pascal Etienne

# Drying of a colloidal suspension deposited on a substrate: experimental and numerical studies

Nathalie Olivi-Tran, Laurent Bonnet, Pascal Etienne

[1] *Universite de Montpellier ,*

*Laboratoire Charles Coulomb,*

*CNRS UMR 5221, CC 074,*

*place E.Bataillon, F-34095, Montpellier, France*

(Dated: August 16, 2021)

## Abstract

We studied a colloidal suspension of polystyrene beads deposited on a glass substrate. The glass substrate contained either straight rough areas on the borders of an open channel or only straight rough areas. The drying of the suspension was observed with an optical microscope which light bulb acted as an energy source to evaporate the suspension. Moreover, the light bulb of the microscope provided optical pressure due to light. We observed that the colloidal particles where trapped on the rough areas of the substrate and not in the open channel, at the end of the drying process. In order to understand the experimental results, we modelled numerically the drying of the suspension by a Molecular Dynamics program. The forces acting on the substrate by the particles are their weight, the optical pressure due to the light bulb of the optical microscope, the attractive Van der Waals force and the repulsive diffuse layer force. The forces acting between two particles are the attractive Van der Waals forces, the repulsive diffuse layer force, the capillary force. The Gaussian random force (linked to the Brownian motion), the particle liquid viscous drag force (also linked to the Brownian motion) are horizontal and applied on one particle. The relation between the normal forces $N$ (forces acting by the particles on the substrate) and the horizontal forces $F$ is Amontons' third law for friction $F \leq \mu_k N$; in rough areas of the substrate $\mu_k$ is larger than in smooth areas. This explains that particles are trapped in the large roughness areas.

## INTRODUCTION

Since the beginning of the $21st$ century, microfluidics has been drawing increasing interests. Among microfluidics studies, experiments and modelling of colloidal suspensions are becoming more and more numerous.Many studies of colloidal suspensions deal with the self patterning of the colloidal particles during drying. The patterns depend on many different factors: size of the colloidal particles, chemical characteristics of the fluid (pH and ionic concentrations), boundaries of the liquid suspension (if it is a droplet), densities of the colloidal suspension, effect of temperature, effect of the different forces acting on the particles. For example, Liang et al. [1] computed the forces (DLVO forces -Derjaguin-Landau-Verwey-Overbeek) which are applied on colloidal particles in a liquid. Bordin [2] modelled aggregation patterns (self patterning) in a 2d model for colloids as a function of densities of the suspension and as a function of temperature. Ghosh et al. [3] studied the surface wettability of the substrate and its effect on the morphology of the deposited colloidal films. Bevan and Prieve [4] studied the Van der Waals attraction between the substrate and the particles, or inbetween the particles which we also need to compute in our work. Finally Thiele [5] used a mesoscopic hydrodynamic long wave model to explain self pattering and Giorgiutti-Dauphine et al. [6] studied the patterns obtained with the contact lines of water-air-particles at the boundary of the liquid film (if it is a droplet) and with nanometer sized particles. The differences between these studies and ours are explained in the following paragraph.

There is a need to model correctly the process of the drying of dispersions in the domain of particles depositions. Therefore, we study the drying of a liquid film of a colloidal suspension deposited on a substrate containing an open channel with rough areas on its borders or only straight and rough areas without any open channel, under the light of a microscope light bulb. In order to obtain rough areas, we scratched these areas with a diamond pen. We assume that the liquid film has a surface which is planar and parallel to the substrate, and that the width of the film (horizontal size) is much larger than the microscope light beam. The size of the colloidal spherical particles is chosen to be $1\mu m$. This size is intermediate between nanoscale physics and micrometer scale physics.This topography was only studied once (see reference [7]) but with a suspension of faceted particles with a size of $10\mu m$. Moreover, in reference [7], the numerical modelling did not take into account all the forces

that we used in this present study. Indeed, several forces are acting between the particles and the substrate, and inbetween the particles themselves. First of them are the forces resulting from microfluidics: capillary forces [7, 8], Brownian forces and Stokes forces [9]. Second of them are the DLVO forces: van der Waals forces [3] and electrostatic double layer forces [10]. Third of them are the optical forces [11] which result from the irradiance of the light bulb of the microscope. Fourth of these forces are the friction forces which differ depending on where are located the particles: in the rough areas of the substrate or in the smooth areas of the substrate. And the fifth force is the weight of the particles. Plus, the $pH$ of the suspension was neutral, the temperature was constant and we studied two suspensions densities.

Experimentally, after the drying of the colloidal suspension, the particles are mainly located on the rough parts of the substrate. Even when the open channels are deeper than the diameter of the particles, these particles do not stay in these channels once all the liquid is evaporated (except few particles).

Numerically, we computed all the forces acting on the particles. From now on, no numerical study of the drying of a colloidal suspension film dealt with all the forces mentioned above.

In section II, we present the experimental process of the drying of a liquid suspension of colloidal particles.Section III deals with the numerical method employed (Molecular Dynamics). And finally section IV shows the experimental and numerical results with a comparison between them.

## EXPERIMENTAL PROCESSES

We study the pattern formation of spherical colloidal particles in an aqueous suspension, when the suspension is dried on a flat substrate with defects. The defects are rough areas of the substrate and micrometer sized open channels .

The experimental suspension is made of dark red $5\%wt$ micro particles based on polystyrene (PS) in an aqueous suspension (Sigma Aldrich). The particles are spherical colloidal particles with a mean diameter $d = 1\mu m$. We used two different dilutions of the initial particles concentration: the first diluted suspension is obtained by adding $1.5cm^3$ of deionized water to $0.05cm^3$ of colloidal suspension, the second diluted suspension is obtained

by adding $3cm^3$ of deionized water to $0.05cm^3$ of colloidal suspension. For the first diluted suspension, the number of particles per volume unit is equal to $8.5.10^{10} \pm 0.05.10^{10} cm^{-3}$ for the second diluted suspension, the number of particles per volume unit is equal to $1.67.10^9 \pm 0.03.10^9 cm^{-3}$. The $pH$ of the suspension was equal to 7.

We deposit the aqueous suspension on a microscope slide (a Borosilicate glass substrate with dimensions $75mm \times 25mm \times 1mm$). The suspension was extended on the glass substrate and we waited 20 $min$ in order that the depth of the suspension was homogeneous. We obtained a liquid film of $5 \pm 0.5 \mu m$ depth.

The surface roughness of the PS particles has been plotted in figure 1a. This surface roughness is an AFM (Atomic Force Microscope) scan obtained with Nanosurf Nanite AFM apparatus. The surface roughness of the glass substrate has been plotted in figure 1b and is obtained with the same apparatus (AFM) than the surface roughness of the PS particles. The smaller asperities of the spherical particles have a height (peak-to-valley) of $20nm$ with a width of $10nm$ (figure 1a). The smaller asperities of the glass substrate have a height (peak-to-valley) of $20nm$ with a width of $2\mu m$ (figure 1b). In order to obtain the distance between the particles and the substrate, we process as in the article of Bevan [4] (roughnesses of the glass and of PS particles are similar to Bevan's results): the dielectric properties of the liquid film are those of the fluid (water) and the thickness of the liquid film (between the particle and the substrate) corresponds to the peak-to-valley distance ($20nm$). Straightforwardly, the smallest distance (surface to surface) between the particles and the substrate is set to be equal to $20nm$ and the smallest distance between a particle and another particle is also set to be equal to $20nm$ . This will be used in the numerical modeling of the drying of the suspension.

We used an optical microscope (Keyence HTX 7000) in order to visualize the colloidal particles on their substrate. These substrates were scratched with a diamond pen, either with a light pressure or with a larger pressure of the pen on the slide. Figures 2 and 3 represent the two types of defects. Figure 2 shows an open channel of width $350 \pm 5 \mu m$ and of depth $35 \pm 3 \mu m$ obtained with a large pressure of the diamond pen. As may be seen in figure 2, the borders of the channel are higher (red area) and may be modelled numerically by an open channel with rough borders. We used the more concentrated suspension on this substrate ($8.5.10^{10} cm^{-3}$). Figure 3 shows three stripes obtained with a light pressure of the diamond pen. These three stripes have a depth and a width of $1 \pm 0.2 \mu m$ each and may be

modelled by a straight linear area of width $1 \pm 0.2\mu m$ where roughness is much larger than in the flat and smooth areas of the substrate. In this last case, there is no open channel, only rough areas and we used the less concentrated suspension on this substrate ($1.67.10^9 cm^{-3}$).

The microscope is equipped with a light bulb made of LED with a spectral irradiance as a function of wavelength plotted in fig. 4 [12]. The light bulb acts on the colloidal suspension in two ways: the first way is the evaporation of the water composing the suspension due to the power of light (coming from the light bulb and with a value of $10 Watts$), the second way is the optical pressure applied by the light on the colloidal particles. The width of the liquid film is much larger than the width of the optical beam, hence we did not take into account the contact line on the borders of the liquid film. And finally, the substrate remains horizontal and the upper surface of the liquid film is also horizontal and parallel to the substrate.

## NUMERICAL MODEL

We modelled numerically the drying of a colloidal suspension over a plane substrate with rough and smooth areas and with an open channel, by Molecular Dynamics. The Molecular Dynamics program uses a predictor corrector method in order to compute the forces, accelerations, velocities and positions with respect to time. The Molecular Dynamics simulations were performed at constant temperature (330K) to solve Newton's equation of motion for each particle. Hence, the trajectories of the particles were computed during the drying process of the liquid film, taking account of the fact that the depth $h$ of the film decreases. The integration time step is $\Delta t = 10^{-7} s$.

In order to fit the experimental data, the parameters employed in the numerical model were the same as the experimental parameters (see table I).

The thin film was numerically modelled by a collection of $N = 600$ spherical particles of equal diameter $d = 1\mu m$ and mass $m$, randomly distributed in a box of length $50d$ in the $x$ and $y$ directions and of height $h = d/2$ in the $z$ direction at the beginning of the computation. On the flat part of the substrate, the particles are moving only in the $x$ and $y$ directions, if the particles are placed in the open channel, they are allowed to move also in the $z$ direction (the numerical process begins when the thickness of the liquid film is equal to the diameter of the colloidal particles). In order to simplify the model, we make the hypothesis

that the particles do not roll but only slide over the substrate. To compute the effect of the liquid film on the particles, the depth $h$ of this film decreases linearly from $h = d/2$ to $h = -10d$ which is the depth of the open channel or from $h = d/2$ to $h = 0$ when there is no channel. The air-liquid interface is characterized by $(x, y, h)$ while the liquid-solid interface is characterized by $(x, y, 0)$ on the flat part of the substrate or by $(x, y, -10d)$ within the channel. Periodic boundary conditions are applied in the $x$ and $y$ directions because we do not take into account the contact lines of the liquid film and the substrate.

Let us compute the different forces which are applied on the particles (the parameters and constants which are used to compute these forces are listed in Table I)

**Vertical forces**

As the particles are identical, their weight is the same for all of them.

The optical pressure which models the effect of the white light (coming from the optical microscope bulb) on the particles is also constant and identical for all particles. With the use of fig.4, we calculate the optical pressure induced by the light of the light bulb within the microscope. The surface area of the shadow (created by the colloidal particle of diameter $d$) is $S = \pi(d/2)^2 = \pi d^2/4 = \pi 10^{-12}/4$. Straightforwardly, the estimated value of the optical force on one spherical particle writes [13, 14]:

$$f_{opt} = n_r.I_f.S/c \tag{1}$$

where $I_f$ is the maximum of the spectral irradiance of the light bulb and $c$ is the speed of light (see fig.4).

The attractive Van der Waals forces between the particles and the plane substrate write [17]:

$$f_i^{vdWps} = -(dA_{132})/(6(r-d)^2) \tag{2}$$

where $r$ is the center to center distance between two colloidal particles ($r-d$ is always larger than $20nm$, see section II) and $A_{132}$ is the Hamaker constant (PS-water-glass).

The repulsive force between the spherical particles and the plane substrate are [19]:

$$f_i^{eps} = \kappa\epsilon d\pi(\phi_1^2 + \phi_2^2 - 2\phi_1\phi_2 \exp(-\kappa(r-d))/(\exp(-2\kappa(r-d)) + 1) \tag{3}$$

where $\kappa$ is the Debye Huckel length, $\epsilon$ is the permitivity of water, $\phi_1$ is the surface potential of PS and $\phi_2$ is the surface potential of glass. This force is electrostatic.

**Horizontal forces**

There is no shear flow of the colloidal suspension (the evaporation of the fluid leads to an homogeneous decrease of the fluid height $h$ all over the sample). Anyway, the fluid is in the laminar state and we focus on the regime of small Peclet numbers (the ratio of shear driven to Brownian motion at the particle scale) and we assume that the Reynold's number of the fluid -water- is small hence there is no convection.

The particles are submitted to attractive Van der Waals forces (forces between two particles) which writes [10] ($r - d$ is always larger than $20nm$, see section II):

$$f_i^{vdWpp} = -(dA_{131})/(24(r-d)^2) \tag{4}$$

where $A_{131}$ is the Hamaker constant (PS-water-PS). The particles are also submitted to repulsive electrostatic forces (forces between two particles) which write [19]:

$$f_i^{epp} = \kappa\epsilon(d/2)(\phi_1)^2(\exp(-\kappa(r-d))/(1+\exp(-2\kappa(r-d))) \tag{5}$$

Particles which are not located in the channel but on the flat part (smooth or rough) of the substrate are subjected to lateral capillary forces (forces between two particles). These forces are attractive and are written [7, 8, 18]:

$$f_i^c(r) = -\pi\gamma r_c^2 \sin(\phi_c)^2 \frac{d}{(r-d)^2} \tag{6}$$

where $r_c$ is the radius of the liquid solid contact line on the spherical particles, $\phi_c$ is the mean slope angle of the meniscus at the contact line (also on the spherical particles), $\gamma$ is the surface tension of water and $R = d/2$ . Figure 5 shows a schematic description of these parameters. The analytical expressions of $r_c$ and $\phi_c$ are written [7, 8, 18]:

$$r_c = (h(d-h))^{1/2} \tag{7}$$

$$\phi_c = \arcsin(\frac{2r_c}{d}) - \alpha \tag{8}$$

where $\alpha$ is the wetting angle at the three contact line (liquid-particle-air).

The particles are submitted to Brownian motion which is linked to a viscous drag force according to the fluctuation-dissipation theorem. Hence, to compute the Brownian motion we use a Gaussian random force which is expressed through the formalism of Wiener [7, 9]:

$$f_i^b(t) = \sqrt{6\pi k_B T h \eta}\Delta W(t) \tag{9}$$

where $\Delta W(t)$ is computed with a Gaussian random number as $< \Delta W(t) >= 0$ and $< \Delta W(t)\Delta W(t') >= \Delta t$. This force is applied on one particle by the surrounding fluid and depends on $h$. Here $k_B$ is the Boltzmann constant, $T$ the temperature and $\eta$ the viscosity of water.

The particle liquid viscous drag force is computed with the Stokes formalism [7, 9]:

$$f_i^S(t) = -3\pi h\eta v_i(t) \tag{10}$$

where $v_i(t)$ is the speed of the particle. This force is also applied on one particle by the surrounding fluid and depends also on $h$.

**Relation between horizontal and vertical forces**

Finally,we deal with the friction force induced by the roughness of the substrate. We make the hypothesis that the particles do not roll but only slide on the substrate and thus are submitted to friction forces. The vertical forces $N$ applied on the particles are the weight, the optical pressure,the van der Waals force and the diffuse layer (electrostatic) force. Straightforwardly, the kinetic friction force is opposed to the horizontal component of the forces applied on the particles. As long as the sum of the horizontal forces $f_i^h$ obeys the following equation Coulomb's law of friction called also Amontons' third law:

$$|f_i^h(r)| \leq \mu_k N \tag{11}$$

where $\mu_k$ is the kinetic friction coefficient (for particles in motion parallel to the substrate) which is multiplied by the normal force $N$ (obtained with the weight, the optical pressure, the van der Waals force and the diffuse layer force between particles and substrate). There is no literature on the values of the kinetic friction coefficients which simulate the friction of PS on smooth areas of glass or which simulate the friction of PS on rough areas of glass. Therefore, we chose a large value (see table I) of $\mu_k$ for rough areas and a small value for smooth areas.

When equation 11 is valid, one has to add a friction force to all the forces which act on a particle (this friction force has a norm equal to $|f_i^h(r)|$ with an opposite direction). For large roughnesses ( $\mu_k = 0.9$, see table I) the horizontal forces applied on one particle are multiplied by 0.1 hence the displacement of the particle is small in this case and the particle

remains close to the rough area. In the case of smooth areas ($\mu_k = 0.3$, see table I), the horizontal forces are multiplied by 0.7, hence the particle can move on these areas (larger displacements). When equation 11 is not valid, the horizontal forces remain unchanged for rough and smooth areas (we do not add the friction force to all the forces applied to one particle).

## RESULTS AND DISCUSSIONS

The experimental results which show the patterns obtained when the colloidal suspension is dried are represented in figures 6 and 7. By comparing the substrate with rough areas and with an open channel (figure 2) with the equivalent substrate with the dried colloidal suspension (figure 6), one may see that particles are trapped in the rough areas but not in the open channel (except a few particles). Similarly, by comparing the substrate with rough areas (figure 3) and without open channel with the dried suspension on the equivalent substrate, one may see again that the particles are sticked to the locations where the roughness is higher (figure 7). Figure 3 has less rough areas than figure 7 but both have rough straight areas where particles are trapped (the number of stripes obtained with a light pressure of the diamond pen depends on the wear of the pen). In figures 6 and 7, particles which are not located in the rough areas are randomly distributed in the smooth areas of the substrate. In order to understand the mechanisms which lead to these results, we modelled the drying of the colloidal suspensions on substrates with a large channel and/or rough areas. Thus, we used a Molecular Dynamics program.

The weight of each spherical particle is equal to $4/3\pi(d/2)^3.\rho.g = 5.39.10^{-18}N$ (see table 1 for the values and definition of the parameters).

The maximum of $I_f$ (spectral irradiance) is equal to $1200.10^7 W/m^3$ (see fig.4). So the value of the optical force is $1200.10^7(\pi/4)10^{-12}/(3.10^8) = 5.02.10^{-11}N$ for each particle (see equation 1).

The value of the attractive van der Waals force between the particle and the substrate is calculated with equation 2, and yields the value of $f_{vdw} = 1.25.10^{-11}N$. The value of the repulsive force due to the electrostatic diffuse layer between the particle and the substrate is calculated with equation 3, this force is equal to $1.13.10^{-11}N$ (assuming that the surface to surface distance is equal to $20nm$, see figure 1a and 1b and section II).

Thus, the normal forces applied on the substrate by a particle is obtained by adding all the attractive forces and by subtracting the repulsive forces calculated above and equal $5.14.10^{-11}N$.

In order to model the effect of friction on the patterning of the colloidal particles, we computed all the horizontal forces acting on these particles (see figures 8 and 9). One may see in figure 8 that capillary forces and electrostatic diffuse layer forces are dominating (for the case where there is an open channel in the substrate). But in figure 9 (for the case where there are only rough straight areas in the substrate), only capillary forces are dominating. This is explained by the fact that particles which are located in the open channel are not subject to capillary forces (particles are completely surrounded by the fluid, with a depth $0 > h > -10d$)) except at the end of the drying process, so the sum of all the capillary forces is smaller when there is an open channel. This can also be deduced from the comparison between figure 8e and figure 9e: the capillary forces differ from a factor 10.

In the computation, if the absolute value of the addition of all horizontal forces applied on one particle obeys Amontons'third law (Coulomb's law), and if the particle is located in a rough area of the substrate, the horizontal forces applied on this particle are multiplied by 0.1. Straightforwardly, the probability for one particle to be trapped in its location is much larger when the kinetic friction coefficient is large (rough areas) than when the kinetic friction coefficient is small (in that case, the horizontal forces applied on this particle are multiplied by 0.7). The results are shown in figures 10 and 11. One may see that most of the particles are trapped in the rough areas in both cases (with or without open channel) and the patterns obtained numerically are the same as the patterns obtained experimentally.

We modelled the effect of evaporation by decreasing linearly the depth of the liquid film $h$ with time $t$ .The effect of evaporation in equations 6,7 and 8 which are functions of the depth of the liquid film $h$, is shown in lateral capillary forces using $r_c$ ($r_c$ is the radius of the liquid solid contact line on one particle),$\phi_c$ (which is the mean slope angle of the meniscus at the contact line on one particle) and $\alpha$ ( which is the wetting angle at the three contact line (liquid-particle-air)). The particle liquid viscous drag force acting on one particle (equation 10) also depends on $h$ as well as the Gaussian random force (equation 9).

In the present study, we gave only one value to each parameter $r_c$, $\phi_c$ and $\alpha$ (see figure 5 and equations 6,7 and 8). It is possible to change the values of these parameters by varying the $pH$, adding surfactants to the suspension and functionalizing the particles: the

contact angle (at the air water interface) changes with the $pH$ [20], and functionalizing the PS particles or adding surfactants to the suspension influence also the capillary forces [21]. Moreover, a higher $pH$ induces increased electrostatic repulsion between particles [21] (see equations 3 and 5 in which the electrostatic repulsion is calculated).

The sizes of the particles (micro or nanoscale) or the polydispersity of the particles influence the self patterning [22, 23]. Indeed, the particles' diameters $d$ act in equations 1 to 8, thus the sizes of the particles are of much importance in selfpatterning processes in general, and in particular in the action of roughness (see equation 11 which takes the sum of all the vertical forces into account, where this sum is multiplied by the kinetic friction coefficient and compared to the sum of all horizontal forces).

The patterns obtained at the end of the drying of the liquid suspension may be analyzed using various methods [24]. But, in our case, the geometrical analysis of the experimental results (see figures 6 and 7) is difficult because of the impossibility to distinguish between different particles.

Finally, when dealing with our modeling and in both cases (substrate with an open channel or substrate without open channel), the vertical forces ($5.14.10^{-11}N$) are larger than the mean horizontal forces (see figures 8 and 9). When comparing with reference [7] which is similar to the present study (but with faceted particles of size $10\mu m$), we observe that we obtain here that particles are trapped in the rough areas like in reference [7]. However, in reference [7] only part of the forces are computed when comparing with the present study. Indeed Lallet et al. [7] calculated only the Stokes forces, the capillary forces and the Brownian forces; moreover, the friction effect was modelled by systematically multiplying the horizontal forces by 0.1 when the corresponding particle was on a rough area (without calculating the relative norms of vertical and horizontal forces). In this study, the vertical optical forces are dominating therefore Coulomb's law applies when computing the horizontal forces (see equation 11). So, the optical pressure has a non negligible effect on the self patterning of colloidal suspensions. Therefore, one has too take into account the spectral irradiance of the light bulb of the optical microscope when studying particles with sizes close to the light's wavelength.

## CONCLUSION

We performed experiments of the drying of an horizontal suspension of micrometer sized colloidal particles on a substrate with rough areas for the first case, and with rough areas and an open channel for the second case. The horizontal width of the suspension was much larger than the width of the optical beam coming from the optical microscope; hence we made the hypothesis that the surface of the fluid is horizontal, parallel to the substrate and that the contact line (between the substrate and the liquid) is far from the optical beam.

To model these experiments we used a Molecular Dynamics program; we took into account all the forces (capillary forces , Brownian forces , Stokes forces, DLVO forces -van der Waals forces and electrostatic double layer forces-, optical forces, friction forces and weight). We did not neglect any force. The effect of evaporation has been also modelled with the decreasing depth of the liquid film: this depth acts on capillary forces, Stokes forces and Brownian forces.

To conclude,

- the patterns obtained experimentally were the same as the patterns obtained numerically;
- we computed all possible forces acting on these colloidal particles;
- we tried to model correctly the process of the drying of dispersions in the domain of particle depositions;
- we calculated the optical pressure applied on particles: this pressure can not be neglected in our case (wavelength of the light -coming from the light bulb of the optical microscope- close to the size of the particles);

These four facts make the originality of our study.

Acknowledgements: All the authors thank the Opto Fluidic Platform of Montpellier (POMM) for providing the experimental results necessary to the writing of this article.

[1] Yu. Liang, N. Hilal, P. Langston, V. Starov *Interaction forces between colloidal particles in liquid: Theory and experiment* Adv. in Coll. and Interface Science, **134** (2007) pp.151-166

[2] J.R. Bordin, *Distinct aggregation patterns and fluid porous phase in a 2D model for colloids with competitive interactions* Physica A **495** (2018) pp.215-244

[3] U. U. Ghosh, M. Chakraborty,A.B. Bhandari,S. Chakraborty,S. DasGupta,*Effect of Surface Wettability on Crack Dynamics and Morphology of Colloidal Films* Langmuir **31** (2015) pp.6001-6010

[4] M. A. Bevan and D. C. Prieve, *Direct Measurement of Retarded van der Waals Attraction* Langmuir **15** (1999),pp.7925-7936

[5] U.Thiele, *Patterned deposition at moving contact lines* Advances in Colloid and Interface Science **206** (2014) pp.399413

[6] F. Giorgiutti-Dauphiné and L. Pauchard, *Striped patterns induced by delamination of drying colloidal films*, Soft Matter, **11** (2015) pp.1397-1402

[7] F.Lallet and N.Olivi-Tran, *Micrometer sized particles in a two-dimensional self-assembly during drying of liquid film* Phys. Rev. E **74** (2006) 061401

[8] J.Aizenberg, P.V.Braun, P.Wiltzius, *Patterned Colloidal Deposition Controlled by Electrostatic and Capillary Forces*, Phys. Rev. Lett. **84** (2000) 2997

[9] D.Pnueli and C.Gutfinger, *Fluid Mechanics* (Cambridge University Press, 1997, Cambridge)

[10] L. N. McCartney and S. Levine, *An Improvement on Derjiaguin's Expression at Small Potentials for the Double Layer Interaction Energy of Two Spherical Colloidal Particles*Journal of Colloid and Interface Science, **30**, No. 3, (1969) pp.345-354

[11] A. Ashkin, *Acceleration and trapping of particles by radiation pressure*, Physical Review Letters, **24**, No. 4,(1970) pp.156

[12] Courtesy of Keyence Research and Development

[13] P. Lebedew, *Untersuchungen über die Druckkräfte des Lichtes*, Annalen der Physik (1901) Series 4 6, pp.433-458

[14] E.F. Nichols, G.F. Hull *The Pressure due to Radiation*, The Astrophysical Journal,(1903) **17** No.5, pp.315-351

[15] T.S.Wong,T.H.Chen, X.Shen, C.M.Ho, *Nanochromatography Driven by the Coffee Ring Effect* Anal. Chem. **83** (2011) pp. 18711873

[16] J.Visser, *On Hamaker constants: A comparison between Hamaker constants and Lifshitz-van der Waals constants* Adv. in Coll. and Interface Science, **3** (1972) pp.331-363

[17] S. Alvo, P. Lambert, M. Gauthier, S. Regnier, *A van der Waals Force-Based Adhesion Model*

*for Micromanipulation* in *Adhesion Aspects in MEMS/NEMS* Journal of Adhesion Science and Technology **24** (2010) Issue 15-16 ,pp. 2415-2428

[18] P.A. Krachelvsky, K.Nagayama, *Capillary interactions between particles bound to interfaces, liquid films and biomembranes* Adv. in Coll. and Interface Science, **85** (2000) pp.145-192

[19] V.H. Chhasatia, Y.Sun, *Interaction of bi-dispersed particles with contact line in an evaporating colloidal drop* Soft Matter, **7** (2011) pp.10135

[20] N.Vogel, L. de Viguerie, U.Jonas, C.K.Weiss and K.Landfester, *Wafer-Scale Fabrication of Ordered Binary Colloidal Monolayers with Adjustable Stoichiometries* Adv. Funct. Mater. **21** (2011) pp. 3064-3073

[21] N.Vogel, S.Goerres, K.Landfester, C.K. Weiss, *A Convenient Method to Produce Close- and Non-close-Packed Monolayers using Direct Assembly at the Air-Water Interface and Subsequent Plasma-Induced Size Reduction*, Macromol. Chem. Phys. **212** (2011) pp.1719-1734

[22] N.Vogel, J.Ally, K.Bley, M.Kappl, K.Landfester and C.K.Weiss, *Direct visualization of the interfacial position of colloidal particles and their assemblies*, Nanoscale **6** (2014) pp.6879-6885

[23] V.Lotito and T.Zambelli, *Self-Assembly of Single-Sized and Binary Colloidal Particles at Air/Water Interface by Surface Confinement abnd Water Discharge*, Langmuir **32** (2016) pp.9582-9590

[24] V.Lotito and T.Zambelli, *Pattern detection in colloidal assembly: A mosaic of analysis techniques*, Adv. in Coll. and Interf. Science, **284** (2020) 102252

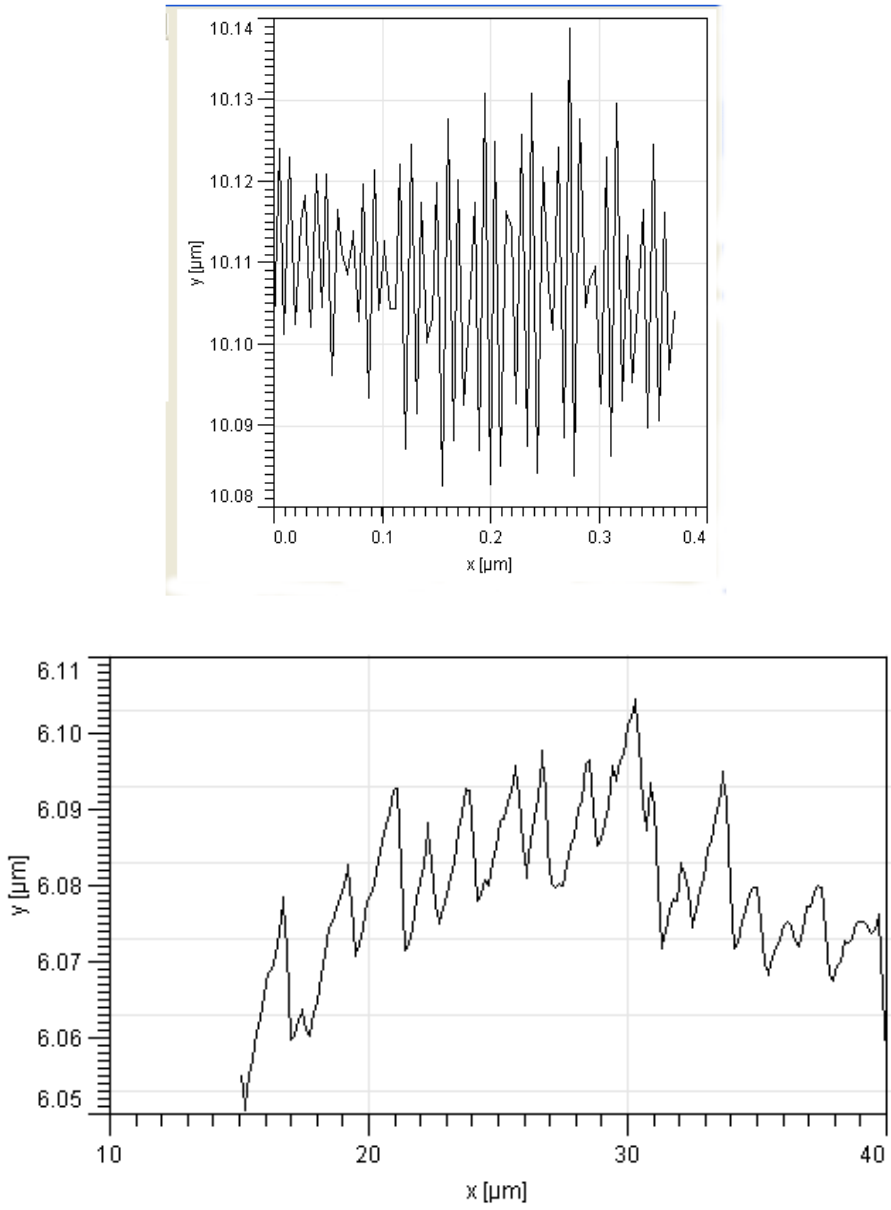


FIG. 1. (top): AFM scan of the surface roughness of a colloidal particle of PS (bottom) AFM scan of the surface roughness of the microscope slide- substrate-

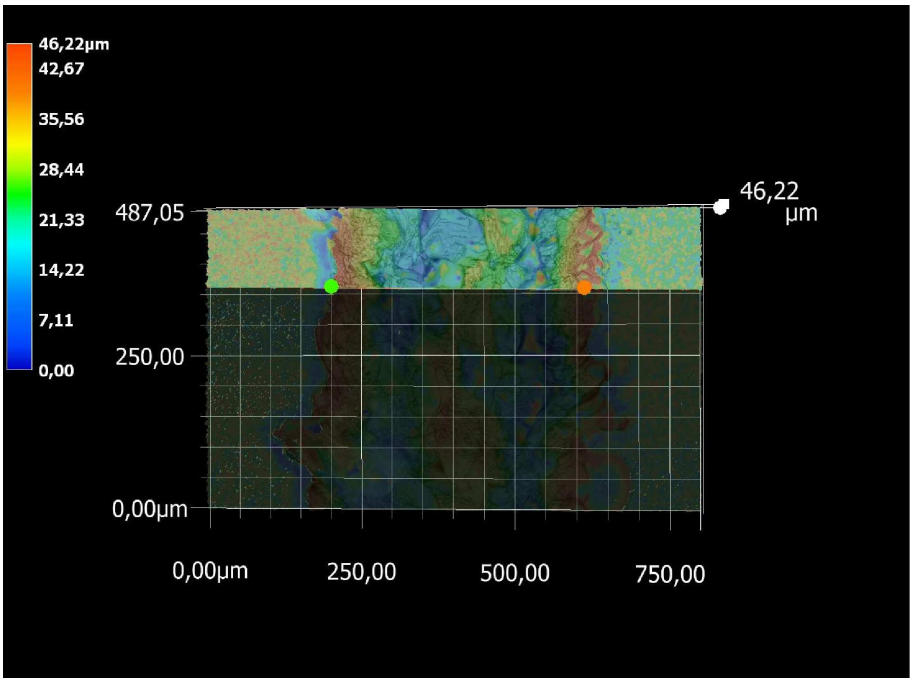


FIG. 2. top view obtained with an optical microscope of the substrate scratched with a large pressure (surface mapping). The stripe (open channel) has a width of $350\mu m$ and a depth of $35\mu m$. The borders of the stripe are higher and present a roughness larger than the non scratched areas of the substrate

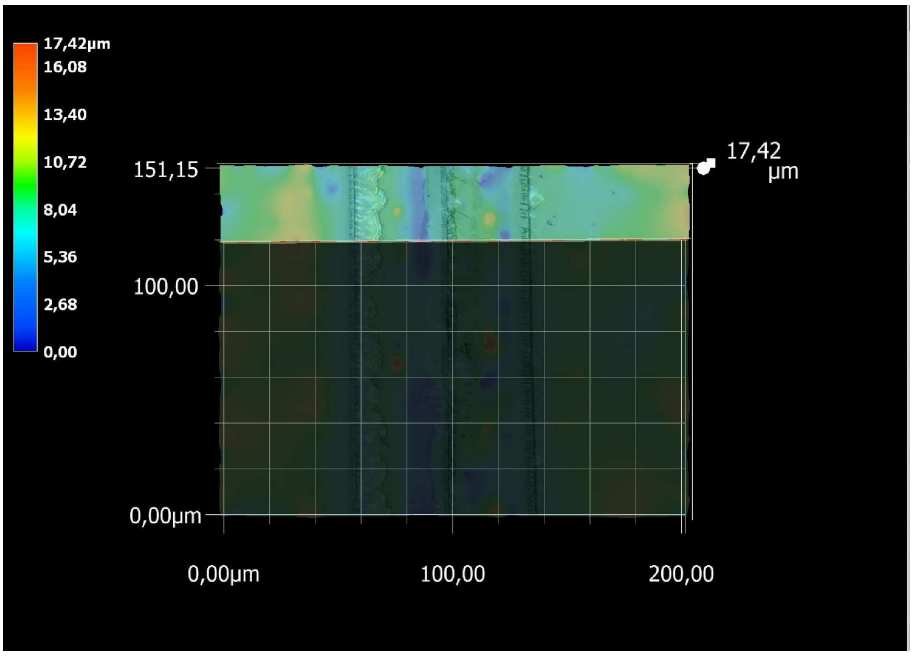


FIG. 3. top view obtained with an optical microscope of the substrate scratched with a light pressure (surface mapping). There are 3 straight areas of width $1\mu m$ and depth $1\mu m$ where the roughness is larger than the non scratched areas

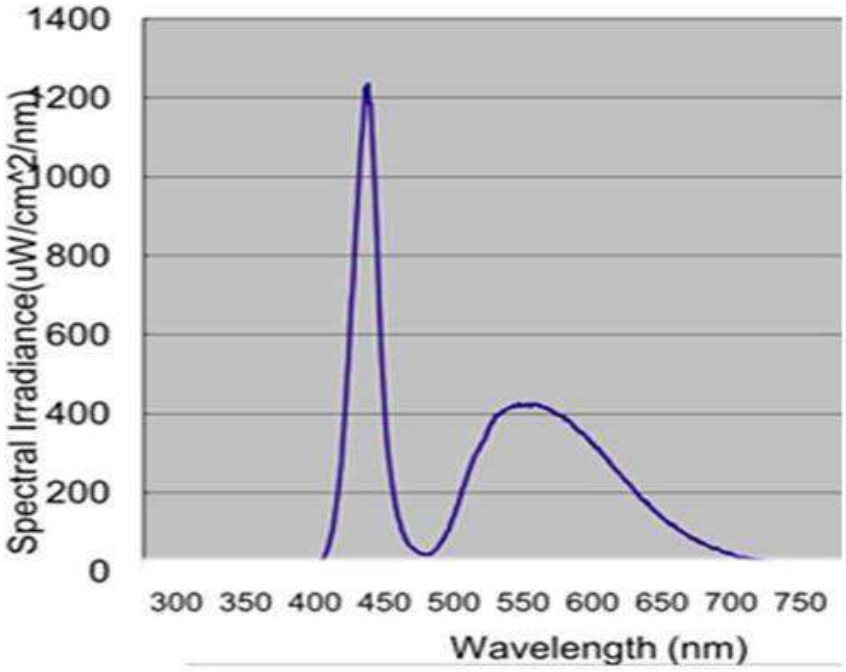


FIG. 4. Spectral irradiance of the light coming from the light bulb of the optical microscope [12]

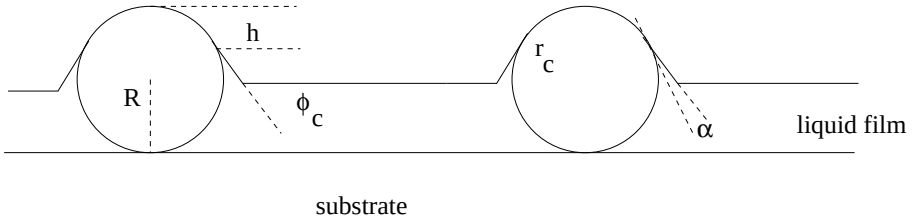


FIG. 5. Scheme of a capillary bridge with all the parameters used in the numerical calculations ($R = d/2$)

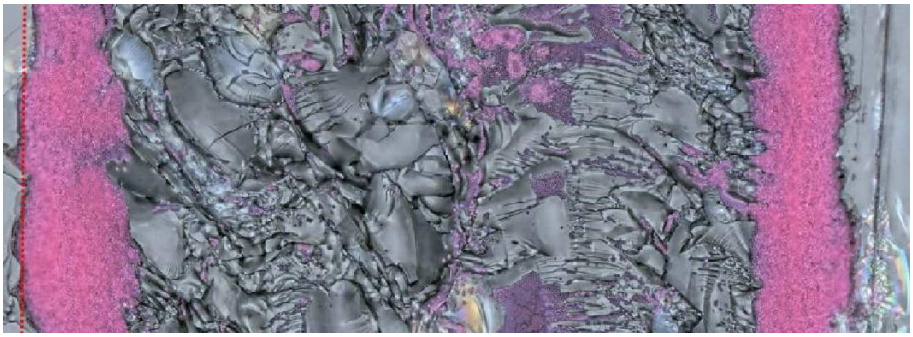

FIG. 6. Top view of a dried liquid film on a substrate containing an open channel bordered by two rough areas. The colloidal particles are trapped on the rough parts of the substrate

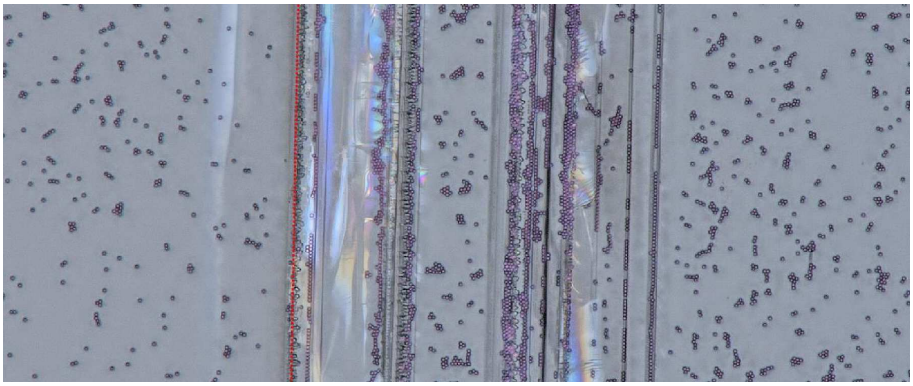

FIG. 7. Top view of a dried liquid film on a substrate with several rough and straight areas of the substrate. The colloidal particles are mainly located on the straight and rough areas.

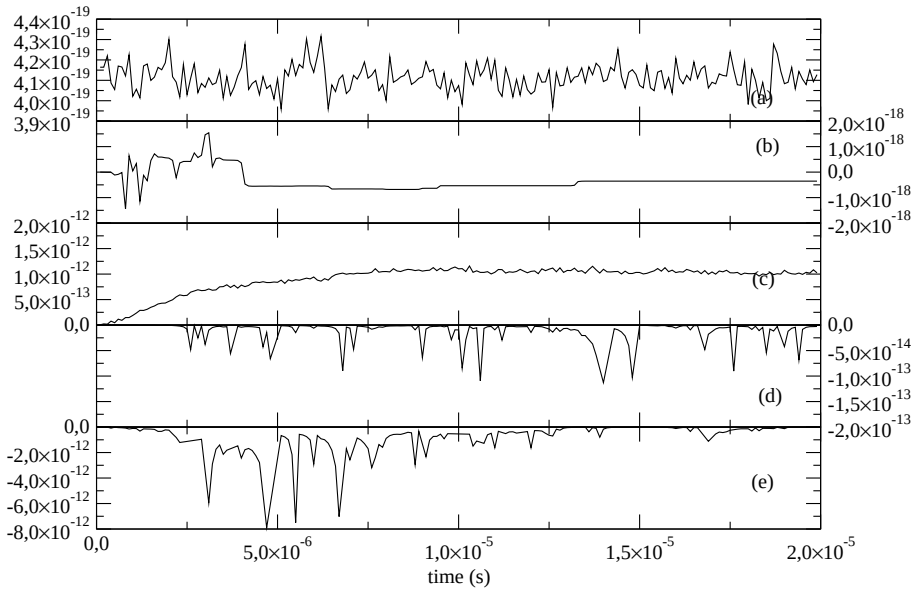


FIG. 8. Plots of the mean forces per particle as a function of time when the substrate contain a deep channel bordered with rough areas (x-axis are in $s$,y-axis are in $N$). (a) Brownian force (b) Stokes force (c) diffuse layer force (DLVO) (d) Van der Waals force (DLVO) (e) capillary force

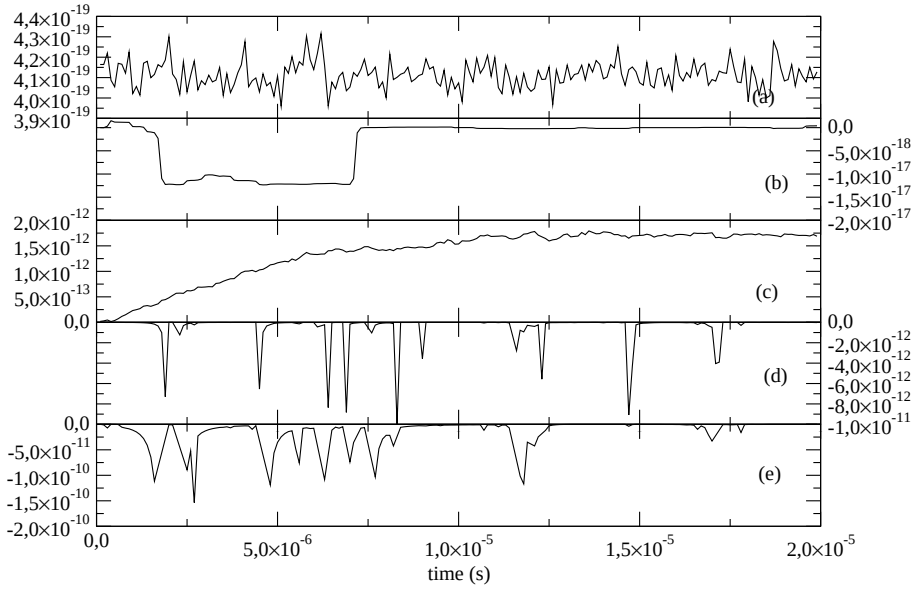


FIG. 9. Plots of the mean forces per particle as a function of time when the substrate contains two straight rough areas (x-axis are in $s$,y-axis are in $N$) (a) Brownian force (b) Stokes force (c) diffuse layer force (DLVO) (d) Van der Waals force (DLVO) (e) capillary force

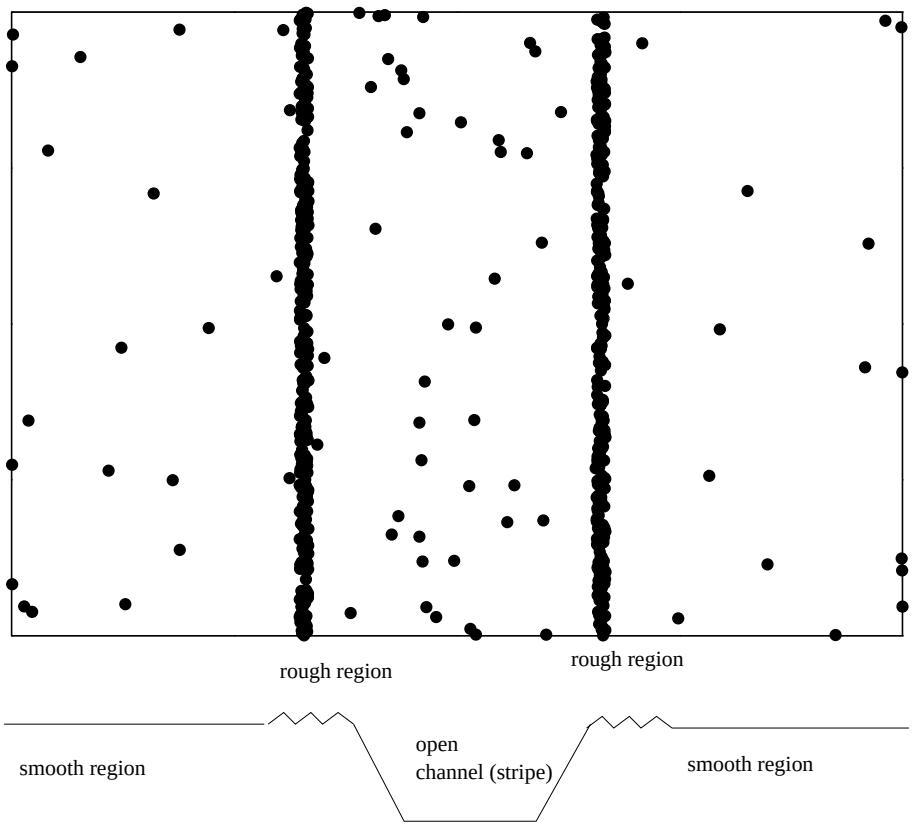


FIG. 10. (top)Top view of the patterns obtained numerically on a substrate with a deep channel bordered with rough areas. (bottom) vertical section of the substrate showing the rough areas and the open channel.

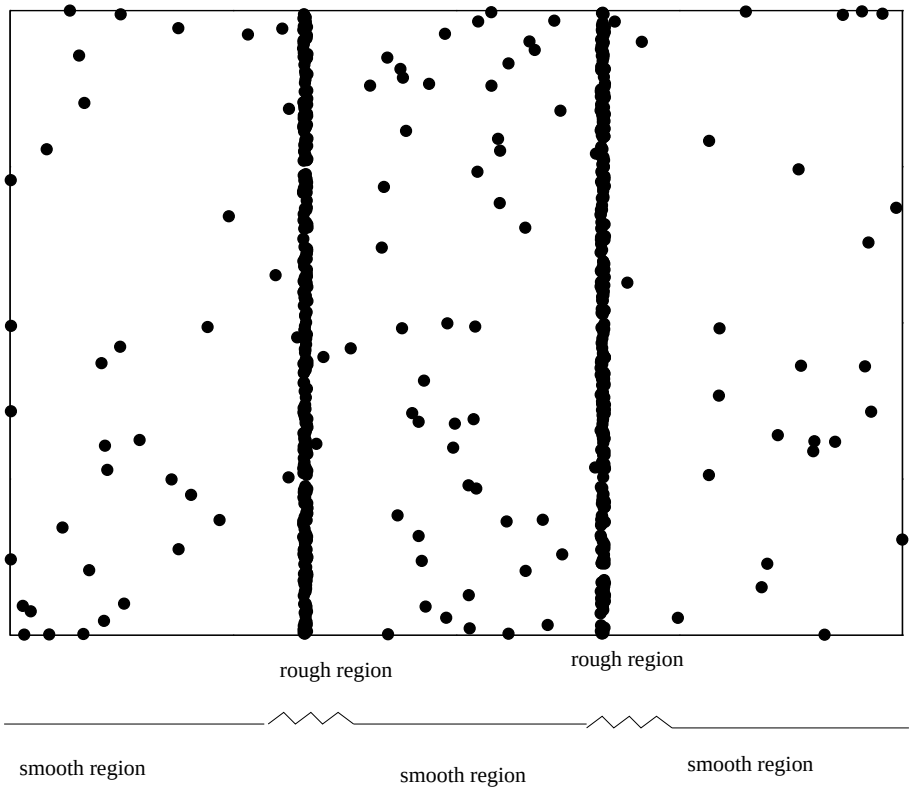


FIG. 11. (top)Top view of the patterns obtained numerically on a substrate with two stripes of larger roughness. (bottom) vertical section of the substrate showing the rough areas

| Name | symbol | value |
|---|---|---|
| density of PS | $\rho$ | 1.05 |
| refractive index of PS | $n_r$ | 1.6 |
| length side of simulation box | $\ell$ | $50\mu m$ |
| particle diameter | $d$ | 1 $\mu m$ |
| thickness of liquid film | $h$ | $d/2$ to $-10d$ $\mu m$ |
| number of particles | $n_1$ | 600 |
| Debye Huckel length | $\kappa^{-1}$ | $(430.10^{-9})^{-1}m^{-1}$ [15] |
| permitivity of water | $\epsilon$ | 78.43 |
| surface potential of PS | $\phi_1$ | $15mV$ [15] |
| surface potential of glass | $\phi_2$ | -40$mV$ [15] |
| Hamaker coefficient (PS-water-PS) | $A_{131}$ | $3.10^{-20}J$ [16] |
| Hamaker coefficient (PS-water-glass) | $A_{132}$ | $10^{-20}J$ [15] |
| gravitational acceleration | $g$ | $9.81m.s^{-2}$ |
| time step | $\Delta t$ | $10^{-7}s$ |
| surface tension of water | $\gamma$ | $73.10^{-3}N.m^{-1}$ |
| wetting angle at three contact line | $\alpha$ | $0.7rad$ [7] |
| temperature | $T$ | $330K$ |
| Boltzmann constant | $k_B$ | $1.3806.10^{-23}m^2.kg.s^{-2}.K^{-1}$ |
| viscosity | $\eta$ | $0.5.10^{-3}kg.m^{-1}.s^{-1}$ |
| kinetic friction coefficient rough areas of substrate | $\mu_k$ | 0.9 |
| kinetic friction coefficient smooth areas of substrate | $\mu_k$ | 0.3 |

TABLE I. Parameters and constants used in the numerical simulations